# Research on Current Outflow in the Plasma Beam of a Low Power Applied-field Magnetoplasmadynamic Thruster

**IEPC-2017-299**

*Presented at the 35thInternational Electric Propulsion Conference*
*Georgia Institute of Technology • Atlanta, Georgia • USA*
*October8 – 12, 2017*

Baojun Wang[1], Haibin Tang[2], Zefeng Li[3], Xin Lu[4], Zhe Zhang[5]
*Beihang University, Beijing, China*

**Abstract:** The distribution of outflow current in the plasma beam of a low power Applied-field Magnetoplasmadynamic (AF-MPD) thruster was measured and evaluated in this work. A Faraday probe was employed to measure the net current in the beam under various applied field strengths and propellant supply proportions. The power of the thruster was varied from 5.5kW to 7.5kW over various operating conditions. The experimental results show that the whole beam can be classified into two regions according to the net current polarity, i.e. a central region where the net current is negative, and an outer region where the net current is positive. Increase of applied field was found to strengthen the net current in the near field (z≤300mm) and make the range of the central region wider. Increase of cathode propellant proportion made the net current weaker in the whole regions. Based upon analysis of the distribution of outflow current, a microscopic interpretation of formation of outflow current is presented in which a radial electric field will be formed in the plasma beam and that field can confine and accelerate the ions.

## Nomenclature

| | | |
|---|---|---|
| $R_a$ | = | Inner diameter of anode |
| $R_c$ | = | Outer diameter of cathode |
| $Ba$ | = | Applied field strength |
| $m_a$ | = | Anode propellant mass flow rate |
| $m_c$ | = | Cathode propellant mass flow rate |
| $I_F$ | = | Net current measured by Faraday probe |
| $r$ | = | Horizontal radial direction |
| $z$ | = | Axial direction |

## I. Introduction

The AF-MPD thruster has the potential to be used as a primary propulsion system in high energy missions[1,2,3] and Near Earth Object (NEO) deflection mission[4]. However, the working mechanisms of AF-MPD thrusters are complex and not fully understood. One of the characteristics of the AF-MPDT is that a fraction of the current between the peripheral anode and axial cathode can extend downstream of the thruster geometry, which means a part of the acceleration interactions take place outside the thruster[1].

Measurement of outflow current in the thruster's plasma beam can provide a useful perspective to understanding the acceleration mechanism of the MPD thruster, and this has been reported in the literature.

[1] PhD Candidate, School of Astronautics, wangbaojun@buaa.edu.cn.
[2] Professor, School of Space and Environment, thb@buaa.edu.cn.
[3] Master Candidate, School of Astronautics, mr.lzf@buaa.edu.cn.
[4] Master Candidate, School of Astronautics, luxin11151196@126.com
[5] PhD Candidate, School of Astronautics, zhangzheplasma@buaa.edu.cn.

Fradkin5 measured outflow current of a lithium fueled MPD arcjet with a Rogowski loop and found that more than 40% of the arc current extended 90-cm downstream of the arc head in some operating conditions; this means that the ambient environment can significantly influence the laboratory thruster,[6,7,8] and the wall of the vacuum tank may interact with the thruster through the outflow current. Schock[9]measured the azimuthal current with a water cooled Hall probe and concluded that the distribution of electromagnetic force in the plasma jet was determined from the outflow current distribution. Myers[10] measured the current distribution in the plume of both self and applied field steady state MPD thrusters operated at power levels between 20 and 250 kW; this was done with a Hall probe that was swept at a high speed to protect the probe from extremely hostile thermal load. It was found that 30% of the discharge current was measured downstream, and it was also found that outflow current can be helpful to explain the temporal variation of the voltage observed under certain operating conditions.

The above noted researchers measured the outflow current precisely, but the measurement techniques are complex and must endure the high temperature environment for extended time. Past researches considered the influence of applied field, but little attention has been paid to the influence of propellant mass flow rate. In this paper, the outflow current was measured with a simple method to determine the influence of applied field as well as propellant supply proportion. The distribution of outflow current in the plasma beam of a 10kW class steady state AF-MPD thruster using argon propellant was examined.

## II. Experiment

### A. Vacuum System

The vacuum system consisted of a vacuum tank, pumping system, electrical control equipment and other peripheral equipment. The vacuum tank was dia.1.8m×3.2m in length. The pumping system consisted of four 2X-70A mechanical vacuum pumps, two ZJP-600 Roots pumps and two K-800 high vacuum oil diffusion pumps. The total pumping speed was 52000L/s. The system achieved a working vacuum of $6.0\times10^{-2}$ Pa, when the total propellant mass flow rate was lower than 25 mg/s.

### B. AF-MPD Thruster

The steady state applied-field MPD thruster employed in the experiment is shown in Figure 1. Argon propellant was supplied both from anode and cathode orifices. The applied magnetic field coils were centered at the cathode tip. The anode was made of molybdenum and the cathode was made of tungsten. The inner diameter of anode was 12mm and the outer diameter of the cathode was 3mm. The discharge current was 150A; terminal voltage varied from 37V to 50V according to operation conditions. The total propellant mass flow rate was always 21mg/s, but the rate of anode mass flow rate ($m_a$) to cathode mass flow rate ($m_c$) was varied in the experiment. The water cooled solenoid coil provided a maximum magnetic field of 0.2T in the central position.

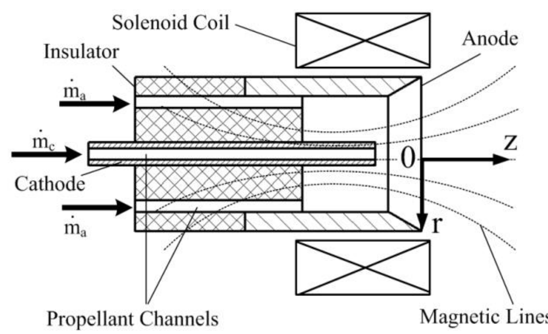


**Figure 1. Structure of the AF-MPD thruster**

### C. Faraday Probe

To measure the outflow current in the plasma beam, a Faraday probe was fabricated as shown in Figure 2. Unlike normal Faraday probes[11], the probe worked without bias voltage and collected electrons and ions together. The collector itself was made of tungsten and had a diameter of 4mm. The collector was covered by a BN guard ring to insulate its flank from plasma. The current flow from the plasma beam to the probe is defined as positive current. The probe was supported with a probe stand as shown in Figure 3; the probe could be moved in an axial direction and radial direction. The axis of probe was parallel to the axis of thruster when measuring the outflow current. The axis of the thruster defines the z-axis and the horizontal radial direction is the r-axis; the coordinate origin is located at the anode exit plane, as shown in Figure 3.

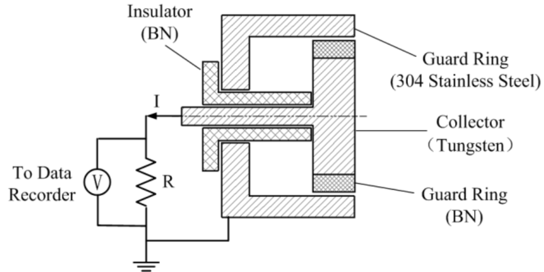


**Figure 2. Structure of Faraday probe**

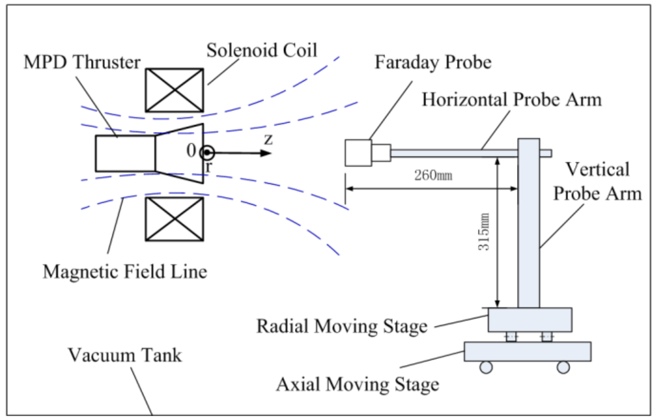


**Figure 3. The layout of probe stand in the vacuum tank**

### D. Outflow Current Measurements

To define the effects of applied field and propellant supply proportion on the outflow current distribution, the experiment was carried out in three steps, as illustrated in Figure 4. The region where z≤300mm is described as near field and the region where z>300mm is far field.

First, to confirm the influence of magnetic field on the current distribution, the probe was moved in the radial direction to measure the near field plasma beam, where the axial position ranged from 100mm to 260mm and the applied field strength varied from 64mT to 127mT. For every operating condition, measurements were made at three different axial positions. As stronger applied fields could push the outflow current to a farther axial position, the axial measurement position was changed with the applied field strength. (More detail of experiment parameters are listed in the Table 1-Part 1.) During data-taking, the probe was moved from the starting point to the terminal point listed in Table 1 with a velocity of 40mm/s, during which data were continually recorded at a frequency of 1k Hz.

Second**,** the axial current distribution in the far field was measured under different magnetic field and propellant supply proportions. Three different operating conditions were employed in this part. The initial operating condition was: Ba=64mT, $m_a$=16.8mg/s, $m_c$=4,2mg/s. Initially, the applied field strength Ba was varied from 64mT to 127mT, with other parameter remaining unchanged. Subsequently, the propellant supply proportion of anode to cathode was varied from 4:1 to 1:4, while the total mass flow rate was kept unchanged and Ba was set at 64mT to keep the initial operating conditions.

Third**,** the current distribution in the near field was measured under different propellant supply proportions. The applied field strength in this part was fixed at 64mT; specific parameters are listed in Table 1.

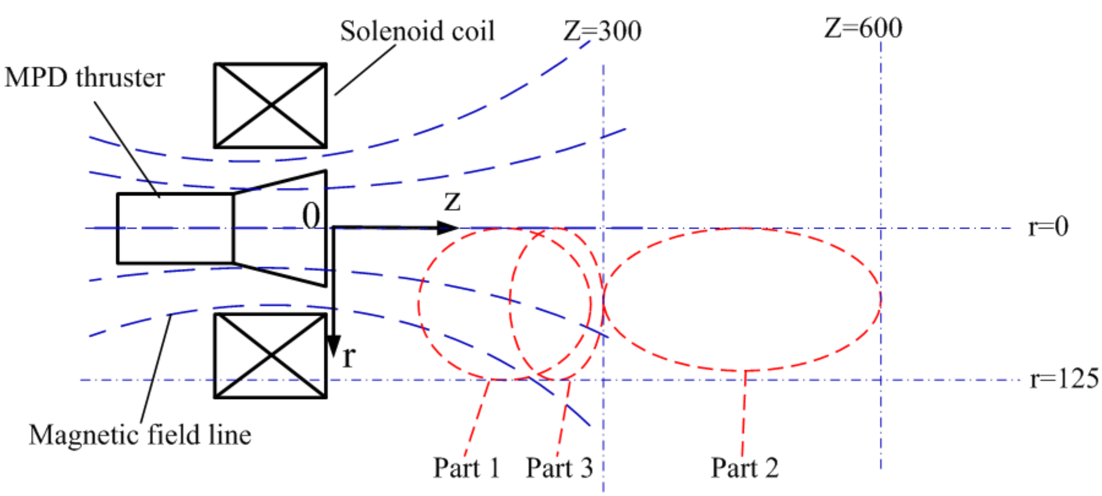


**Figure 4. Sketch map for measuring regions**

**Table 1. Thruster operating conditions and sketch map for the moving path of Faraday probe.**

| | Ba mT | $m_a$ mg/s | $m_c$ mg/s | Starting point r | Starting point z | Terminal point r | Terminal point z | Sketch map for the moving path of Faraday probe |
|---|---|---|---|---|---|---|---|---|
| Part 1 | 64 | 16.8 | 4.2 | 0 | 100 | 125 | 100 | 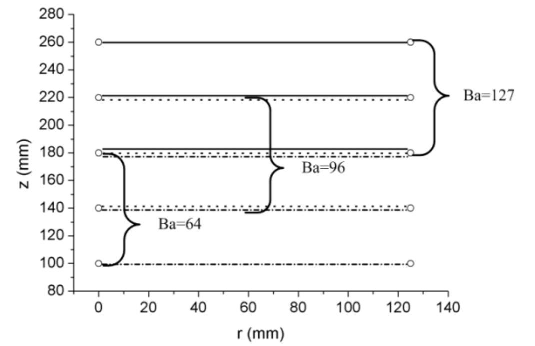 |
| | | | | 125 | 140 | 0 | 140 | |
| | | | | 0 | 180 | 125 | 180 | |
| | 96 | | | 0 | 140 | 125 | 140 | |
| | | | | 125 | 180 | 0 | 180 | |
| | | | | 0 | 220 | 125 | 220 | |
| | 127 | | | 0 | 180 | 125 | 180 | |
| | | | | 125 | 220 | 0 | 220 | |
| | | | | 0 | 260 | 125 | 260 | |
| Part 2 | 64/16.8/4.2 127/16.8/4.2 64/4.2/16.8 | | | 0 | 600 | 0 | 300 | 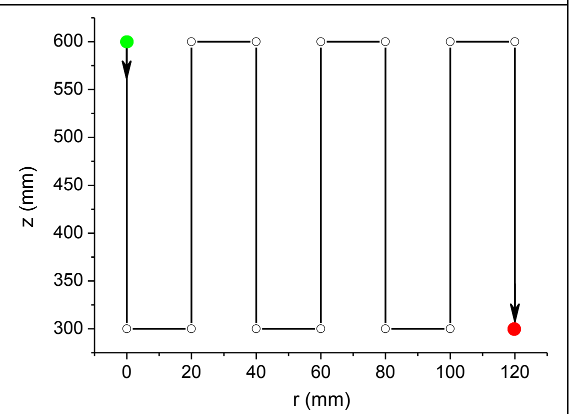 |
| | | | | 0 | 300 | 20 | 300 | |
| | | | | 20 | 300 | 20 | 600 | |
| | | | | 20 | 600 | 40 | 600 | |
| | | | | 40 | 600 | 40 | 300 | |
| | | | | 40 | 300 | 60 | 300 | |
| | | | | 60 | 300 | 60 | 600 | |
| | | | | 60 | 600 | 80 | 600 | |
| | | | | 80 | 600 | 80 | 300 | |
| | | | | 80 | 300 | 100 | 300 | |
| | | | | 100 | 300 | 100 | 600 | |
| | | | | 100 | 600 | 120 | 600 | |
| | | | | 120 | 600 | 120 | 300 | |
| Part 3 | 64 | 16.8/4.2 10.5/10.5 4.2/16.8 | | 125 | 300 | 0 | 300 | 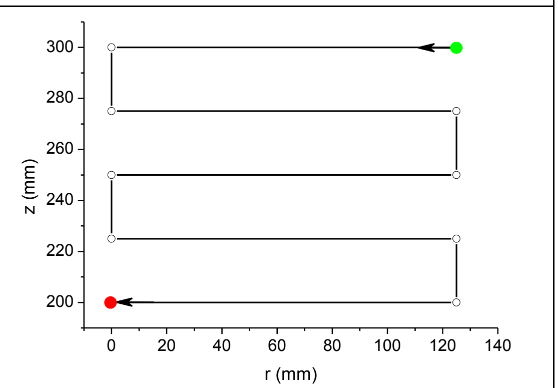 |
| | | | | 0 | 300 | 0 | 275 | |
| | | | | 0 | 275 | 125 | 275 | |
| | | | | 125 | 275 | 125 | 250 | |
| | | | | 125 | 250 | 0 | 250 | |
| | | | | 0 | 250 | 0 | 225 | |
| | | | | 0 | 225 | 125 | 225 | |
| | | | | 125 | 225 | 125 | 200 | |
| | | | | 125 | 200 | 0 | 200 | |





## III. Results and Discussion

### A. Influence of Magnetic Field

Radial variation of outflow current for (a) 64mT, (b) 96mT and (c) 127mT at axial three downstream axial locations are presented in Figure 5;in Figure 5 (d) there is a comparison of the radial variation at z = 180 mm; the axial variation of outflow at different radii for a fixed magnetic field value are shown in Figures 5, € and (f). Several characteristics of these outflows are as follows:

1. All the $I_F$-r curves for radial distribution are unimodal under the operatng condition that $m_a$:$m_c$=4:1.
2. For radial distribution, the net current is negative in the central region and positive in outer region. The boundary of negative current is wider when Ba is stronger.
3. For radial distribution in the near field, higher net current is obtained with stronger applied field. For axial distribution in far field, increasing of Ba makes negative current stronger and makes positive current weaker.

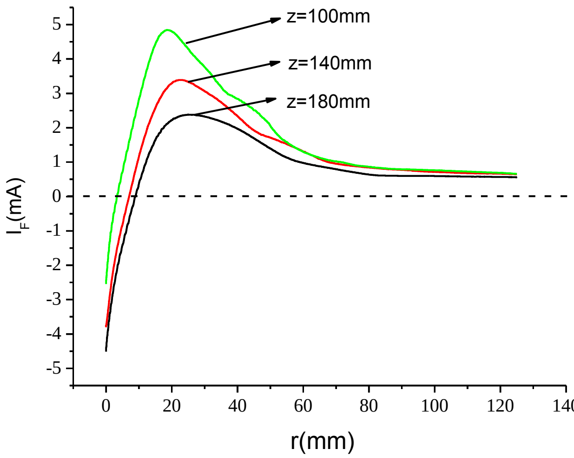


(a) Radial current distribution (Ba= 64mT)

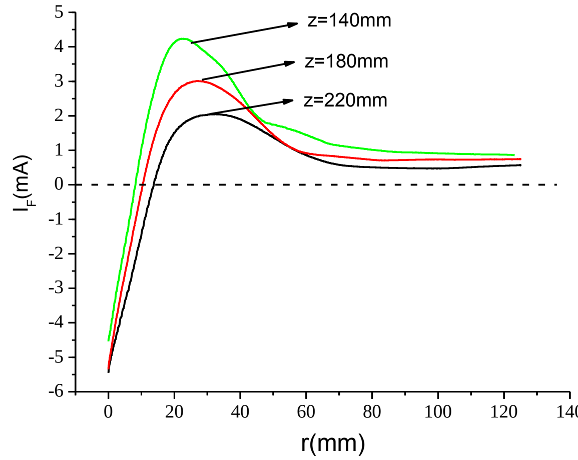


(b) Radial current distribution (Ba= 96mT)

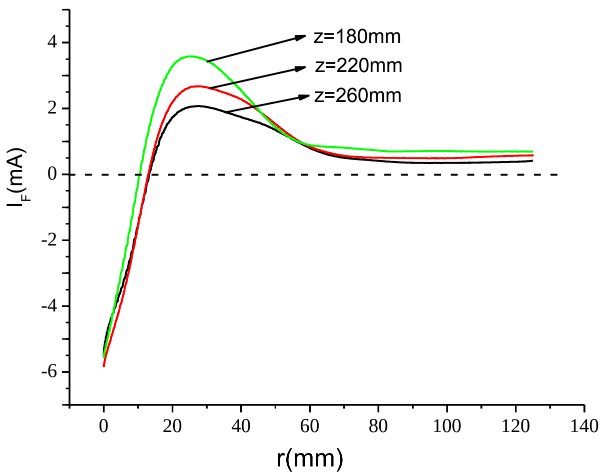


(c) Radial current distribution (Ba= 127mT)

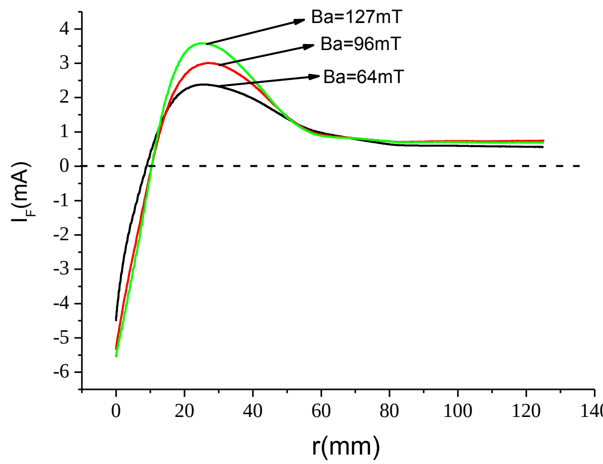


(d) Comparison of radial current distribution under 64mT, 96mT and 127mT (z=180mm)

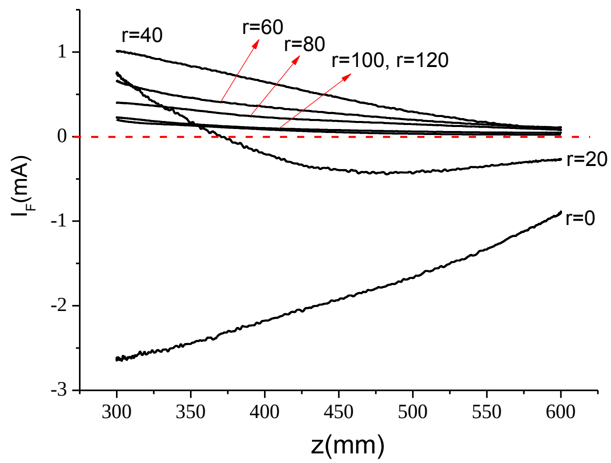


(e) Axial current-distribution (Ba= 64mT)

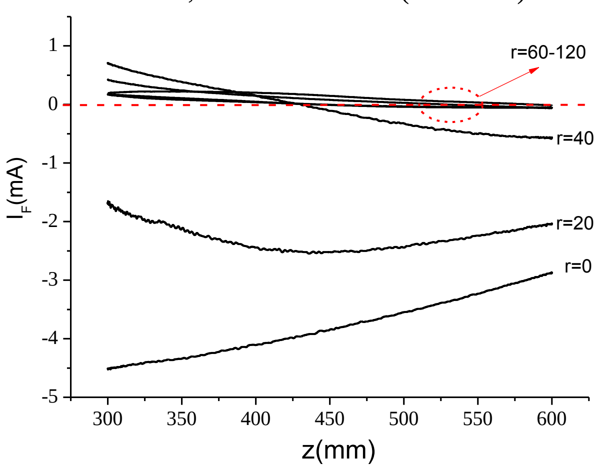


(f) Axial current-distribution (Ba= 127mT)

**Figure 5. Outflow current distribution under different applied field strength**

(Ba=64mT, 96mT and 127mT; $m_a$=16.8mg/s, $m_c$=4.2mg/s;0mm≤r≤125mm, 100 mm≤z≤600mm)

### B. Influence of Magnetic Field and Propellant Supply Proportion

Radial and axial variations of outflow current under different propellant supply proportions are presented in Figure 6. Some characteristics of the variations of the currents can be summarized as:

1. In whole conditions, net current on axes is always negative when z≤600mm.
2. For $m_a$:$m_c$=4:1 and 1:1, $I_F$-z curves are unimodal; for $m_a$:$m_c$=1:4, $I_F$-z curves are bimodal.
3. Increasing of cathode propellant proportion makes the net current in the whole range weaker.

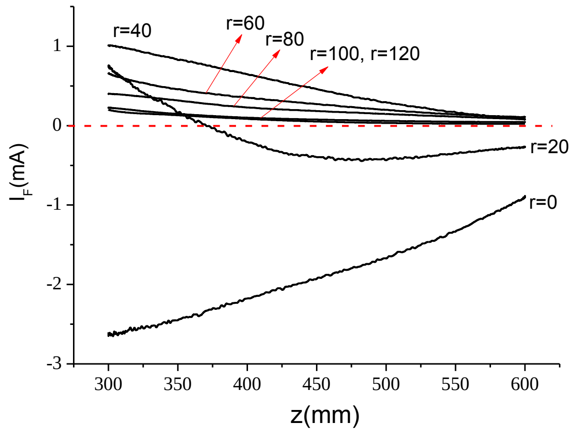


(a) Axial current-distribution ($m_a$:$m_c$=4:1)

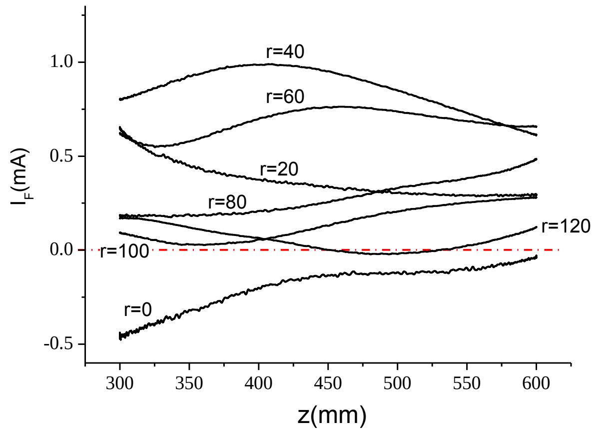


(b) Axial current-distribution ($m_a$:$m_c$=1:4)

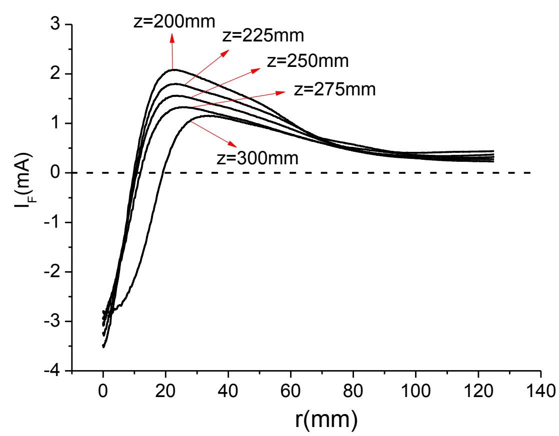


(c) Radial current-distribution($m_a$:$m_c$=4:1)

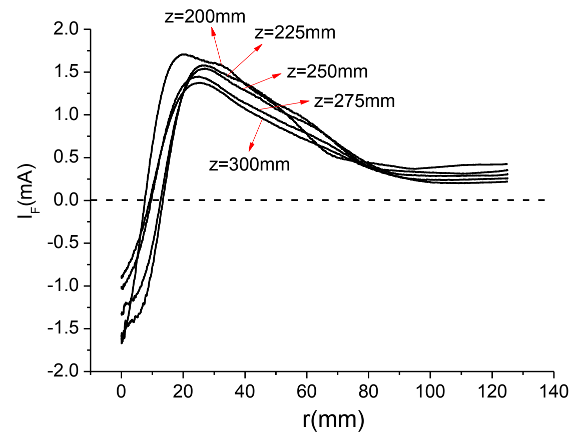


(d) Radial current-distribution($m_a$:$m_c$=1:1)

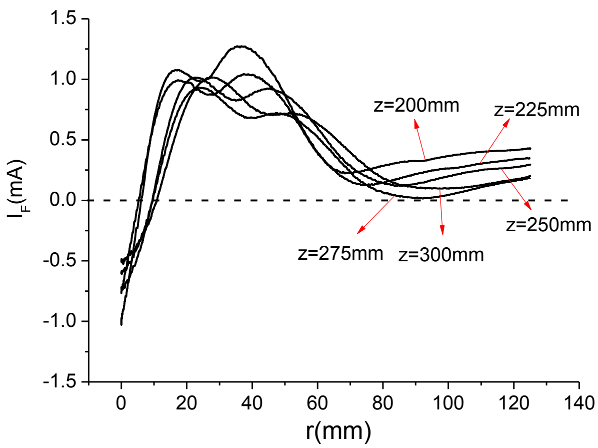


(e) Radial current-distribution($m_a$:$m_c$=1:4)

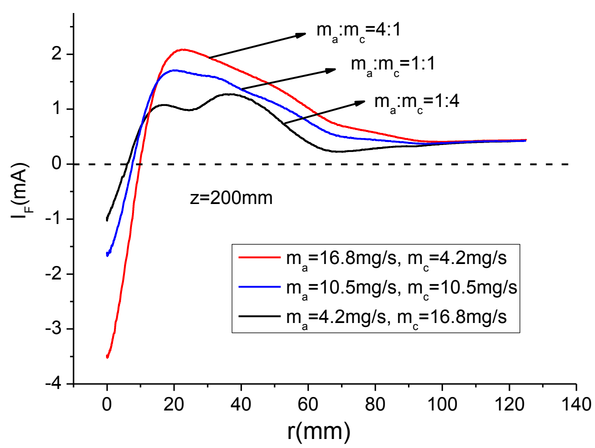


(f) Comparing of radial current-distribution under different propellant proportions

**Figure 6. Current distribution under different propellant proportions of anode to cathode**

(Ba=64mT,0mm≤r≤125mm, 200mm≤z≤600mm)

To make the relationship between the magnetic field and outflow current evident, a nephogram which combines the distribution of net current and magnetic field lines, is shown in Figure 7. The data of current distribution in the figure are obtained from Part 2 and Part 3 of the experiment, where $m_a$=16.8mg/s, $m_c$=4.2mg/s, Ba=64mT, 0mm ≤r≤125mm, 100mm ≤z≤600mm. The nephogram is divided into 20 areas according to the value of net current. The boundary line of negative current and positive current is highlighted with a bold line. The distribution of magnetic field lines is the result of a numerical simulation for the actual solenoid coil parameters of 256 coil turns and coil current of 50A. In the drawing of anode and cathode in the figure, the size is 1:1 to the ordinate.

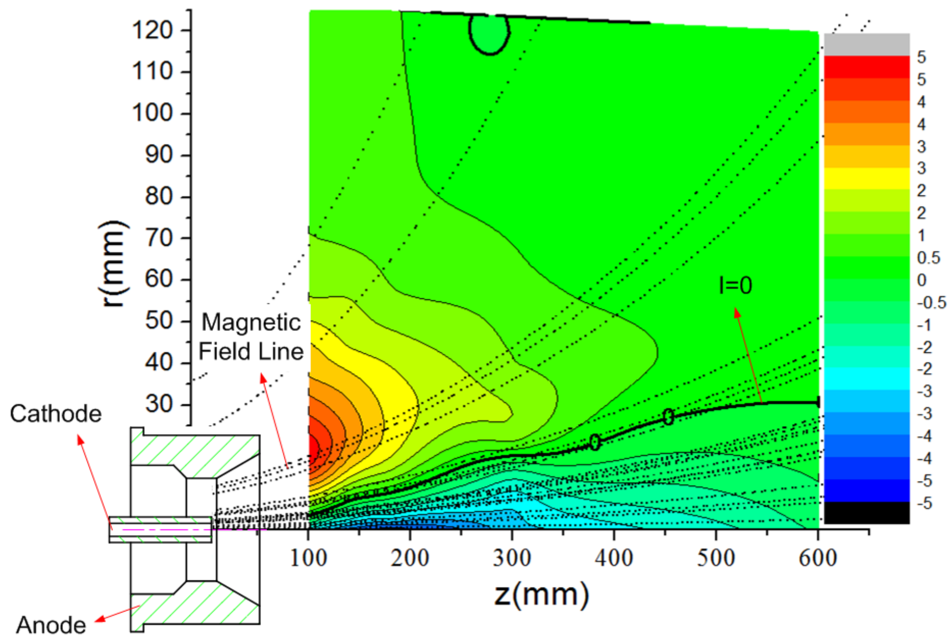


**Figure 7. Distribution of net current and magnetic field**

It can be observed that the negative current is concentrated in the center, the boundary of which agrees well with magnetic field lines. In addition, the magnetic field line crosses over the outer boundary of the cathode, which means the negative current comes from the cathode.

Based on the above observations, a hypothesis can be raised for a microscopic interpretation of outflow current behavior.

First, a large magnitude of electrons are released from the cathode. A part of these are constrained by the magnetic field and will flow downstream along the magnetic field line; this would compose the negative current in the central region. Other electrons would diffuse in the radial direction due to collisions.

Second, electrons diffusing to the anode zone ionize local neutral propellant atoms, forming more free electrons and ions. Most of these electrons are absorbed by the anode, while numbers of ions are left, which compose the positive current in the outer region.

Third, the separation of ions and electrons forms an electric field, the radial component of which can prevent the plasma beam from further diffusing and the axial component of which can accelerate the ions in the outer region.

Finally, in the far field, the applied field is weak so that it cannot constrain the electrons effectively; accordingly, electrons mix with surrounding ions and the net current tends to zero.

The above hypothesis can be applied to propose a phenomenological description of the influence of magnetic fields and propellant proportion on current distribution as follows. The initial electrons are released by the cathode, and are constrained in the central region when they are released. Accordingly, the net current in the central region is main electron current, i.e. negative particle current. This is consistent with the fact that the net current in the central region is always negative. When the applied field is strengthened, more electrons will be constrained, and both the strength and the range of negative current in the near field would increase. Further, positive current at outer region would become larger because of a decrease of electron number density in the outer region. In the far field, where the applied field is very weak, more electrons would escape from the central region, thus the positive current in the outer region would become weaker.

The hypothesis can also be used to explain the influence of propellant proportions. An increase in the proportion of cathode propellant would result in fewer neutral particles in the anode region; this would reduce the source of ions in the outer region. In addition, an increase in cathode propellant would mean increased collisions between electrons and neutral particles in the central region; this would contribute to increased radial diffusion of electrons. As a result, numbers of both ions in the anode region and electrons in the central region are less than before. Thus, an increase in the proportion of cathode propellant can weaken the net current in the whole region.

Consistent with the proposed hypothesis, a part of the initial electrons released by the cathode would be confined in the central region. These electrons can ionize neutral particles and so release more secondary electrons. Most of initial and secondary electrons would be confined by the magnetic field. However, the magnetic field cannot constrain the ions as effectively as electrons, thus many ions can escape from the central region. As a result, the number density of electrons in the central region would be larger than the ions. An electric field would form due to the non-uniform distribution of ions and electrons, as shown in Figure 8. A component of that field can constrain the ions in the outer region and make the beam more concentrated. The axial component points downstream, which can accelerate the ions. Since ions can contribute more thrust than electrons, the field would be beneficial to improving the total thrust of an AF-MPD thruster.

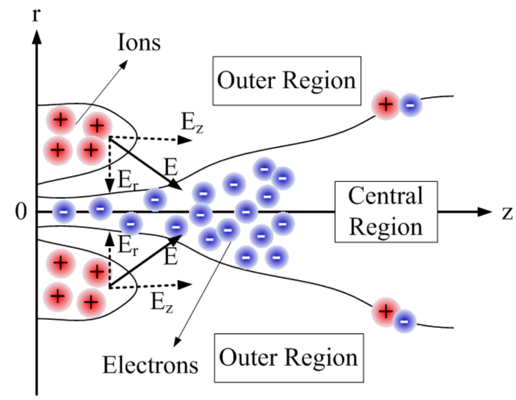

**Figure 8. Distribution of net current and magnetic field**

## IV. Conclusion

This paper has presented measurements of and a model for the distribution of outflow current in the plasma beam of AF-MPD thruster under different applied field strength and propellant supplying proportions. Several characteristics of the outflow current distribution are summarized as follows:

1. The whole plasma beam can be classified into two regions, i.e. the central region and the outer region. The current is negative in the central region and positive in the outer region.
2. An increase of applied field can strengthen the net current in the near field (z≤300mm) and make the range of the central region wider.
3. An increase of cathode propellant proportion makes the net current weaker in the whole regions.

A microscopic interpretation for the formation of outflow current has been given, according to which the central negative current originates from the initial electrons and outer positive current originates from ionized propellant. The separation of ions and electrons caused by an applied field is the primary reason for current out flow, and this is crucial for increasing thrust efficiency, since a radial electric field will be formed in the process and the field can confine and accelerate the plasma beam.

## Acknowledgments

This work was supported by the Fundamental Research Program (No. JCKY2017601C). And we appreciate the helping of Thomas M. York, Emeritus Professor at Ohio State University and Priv. Doz. Georg Herdrich at University of Stuttgart.

## References

[1]Kodys, A., and E. Choueiri."A Critical Review of the State-of-the-Art in the Performance of Applied-Field Magnetoplasmadynamic Thrusters."Aiaa/asme/sae/asee Joint Propulsion Conference & Exhibit 2005.
[2]Arakawa, Y., and A. Sasoh. "Electromagnetic effects in an applied-field magnetoplasmadynamic thruster." Journal of Propulsion and Power; (United States) 8.1(1992):98-102.
[3]Myers, R., M. Lapointe, and M. Mantenieks."MPD thruster technology." (1991):71-90.
[4]Boxberger, A., P. Jüstel, and G. Herdrich."Performance of 100 kW Steady State Applied-Field MPD Thruster."International Symposium on Space Technology and Science 2017.

[5]Blackstock, A. W., et al. "Experiments using a 25-kw hollow cathode lithium vapor MPD arcjet." Aiaa Journal 8.5(1970):886.
[6]Monika Auweter-Kurtz, Gerd Kriille, Helmut Kurtz ,The Investigation of Applied-Field MPD Thrusters on the International Space Station, IEPC-97-116
[7]Connolly, D. J., and R. J. Sovie."Effect of background pressure on magnetoplasmadynamic thruster operation." 7.3(1970):255-258.
[8]Burkhart, J. A., et al. "Low environmental pressure MPD arc tests. "Aiaa Journal 6.7(1967):1271-1276.
[9]Schock, W. "Diagnostics and interpretation of the electrical current distribution in an MPD-thruster."Electric Propulsion Conference 2006.
[10]Myers, R. "Plume characteristics of MPD thrusters - A preliminary examination." (1989).
[11]Zhang, Z., et al. "Calibrating ion density profile measurements in ion thruster beam plasma." Review of Scientific Instruments 87.11(2016):387.